

# ZnO Schottky diodes with iridium contact electrodes

S J Young<sup>1</sup>, L-W Ji<sup>2</sup>, S J Chang<sup>1</sup>, Y P Chen<sup>1</sup> and S-M Peng<sup>2</sup>

<sup>1</sup> Institute of Microelectronics & Department of Electrical Engineering, National Cheng Kung University, Tainan 701, Taiwan, Republic of China

<sup>2</sup> Institute of Electro-Optical and Materials Science, National Formosa University, Yunlin 632, Taiwan, Republic of China

E-mail: lwji@seed.net.tw and lwji@nfu.edu.tw

Received 30 January 2008, in final form 13 May 2008

Published 11 July 2008

Online at [stacks.iop.org/SST/23/085016](http://stacks.iop.org/SST/23/085016)

## Abstract

Schottky diodes with iridium (Ir) contact electrodes on ZnO films were fabricated and characterized in this work. The Schottky barrier height between Ir and ZnO was determined to be  $0.824 \pm 0.04\%$ ,  $0.837 \pm 0.04\%$  and  $0.924 \pm 0.04\%$  eV by the thermionic emission model, the Norde model and capacitance–voltage measurement, respectively. It was also found that the ideality factor of the fabricated ZnO-based Schottky diode was 1.68.

(Some figures in this article are in colour only in the electronic version)

## 1. Introduction

ZnO is a direct wide band gap material that is sensitive in the ultraviolet (UV) region [1, 2]. Its large exciton binding energy of 60 meV and a wide bandgap energy of 3.37 eV at room temperature make ZnO a promising photonic material for applications of light emitting diodes (LEDs), laser diodes (LDs) and UV photodetectors [3–5]. High quality ZnO epitaxial layers can be grown by metal–organic chemical vapor deposition (MOCVD) [1], molecular beam epitaxy (MBE) [6] and pulsed laser deposition (PLD) [7] onto ZnO [2], sapphire [8] and epitaxial GaN substrates [9]. Recently, it has been shown that it is possible to achieve ZnO epitaxial layers with high electron mobility by multi-step PLD [7]. It has also been found that the saturation velocity of ZnO is higher than that of GaN [10]. Furthermore, it has been reported that ZnO is less susceptible to irradiation effects than GaN [10]. Thus, ZnO-based optoelectronic devices are potentially useful for high-speed operation.

Investigation of the metal–semiconductor contact plays a key role in ZnO device application. It is important to achieve a large Schottky barrier height at the metal–semiconductor interface for high performance UV photodetectors. A large barrier height will lead to small leakage current and high breakdown voltage, and will improve the photoresponsivity and the photocurrent to dark current contrast ratio. To obtain a large Schottky barrier height on ZnO, we can choose some metals with high work functions. Many reports have been

published about Schottky contacts on ZnO to date [4]. Sheng *et al* employed Ag as Schottky contact on ZnO films [11]. Ip *et al* reported Pt Schottky contacts on n-type ZnO [12]. Both Mosbacher *et al* and Angadi *et al* promote the same idea to use oxygen plasma treatment on ZnO films and a conversion from ohmic to rectifying behavior is observed for Au contacts on ZnO [13, 14]. However, many of the high work function metals are still not stable at high temperatures, and severe inter-diffusion might occur at the metal–ZnO interface. Iridium (Ir) is an interesting material that has been used as a stable Schottky contact on GaN [13–15]. Furthermore, Ir is also a good conductor with superior thermal and chemical stabilities. GaN-based UV metal–semiconductor–metal photodetectors with IrO<sub>2</sub>, and GaN Schottky diodes with oxidized Ir/Ni Schottky contacts have also been demonstrated in the past [15–17]. However, neither the properties of Ir contacts on ZnO nor the characteristics of ZnO-based devices with Ir contacts can be found so far. In this work, we report on the fabrication of ZnO-based Schottky diodes with Ir contact electrodes. The Schottky barrier height between metal Ir and semiconductor ZnO and the related ideality factor are also discussed.

## 2. Experiment

The ZnO films used in this study were all grown on sapphire (0001) substrates by using radio-frequency sputter (rf sputter) deposition. Rf sputtering is a promising technique for the growth of oxide materials including ZnO, which allows a

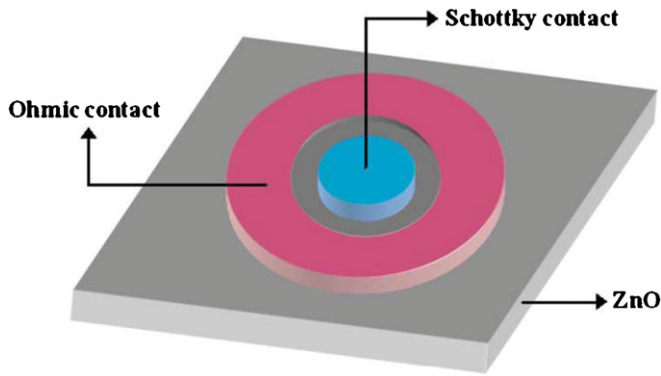


**Figure 1.** Schematic structure of ZnO Schottky diode. The Ir Schottky contact is the inner circle while the Ti/Al/Ti/Au ohmic contact is the outer ring.

low-temperature deposition of films with good crystal quality and electrical properties. A sapphire substrate was placed on the top of an anode, which was 50 mm from the ZnO target of 3 inch diameter. During the growth, the working pressure of the chamber was  $\sim 5.0 \times 10^{-2}$  Torr while the rf power was 200 W and the ratio of  $O_2/Ar$  gas flow was maintained at 1/10. No substrate heating and bias were applied during the deposition. The thickness of the undoped ZnO film was 1000 nm. Sequentially the ZnO films were annealed at 600 °C for 30 min under atmosphere. The as-grown ZnO films were then characterized by x-ray diffraction (XRD) and Hall measurements.

After deposition of the ZnO films, the ZnO Schottky diodes were then fabricated by the standard photolithography and lift-off methods. Ti/Al/Ti/Au (20/60/20/50 nm) as an ohmic contact was first deposited by thermal evaporation and then was annealed at 525 °C for 3 min under  $N_2$  ambient. Then, a 30 nm thick Ir Schottky contact was patterned and deposited by using an E-beam evaporator. The schematic structure is as shown in figure 1, the width of the outer ring (ohmic contact region) is 300  $\mu m$ , and the diameter of the Schottky contact is 250  $\mu m$ . The gap between the Schottky contact and ohmic contact is 25  $\mu m$ .

Current–voltage characteristics of the fabricated devices were measured by an HP 4155B semiconductor parameter analyzer. An HP 4284A precision LCR meter controlled by a Keithley 4200 was employed in characterizing capacitance–voltage properties.

### 3. Results and discussion

By room temperature Hall measurements, it was found that carrier concentration and mobility of the as-grown ZnO films were  $10^{13} \pm 25\% \text{ cm}^{-3}$  and  $70 \pm 15\% \text{ cm}^2 \text{ V}^{-1} \text{ s}^{-1}$ , respectively. It should be noted that we measure several times and obtain similar results each time. This property of our ZnO film is similar to Maeda's result [18]. Figure 2 shows the measured XRD spectrum of the 1000 nm thick ZnO films prepared on the sapphire substrate. We observed a ZnO (002) reflection peak at  $2\theta = 34.24^\circ$ . The peak occurred at  $2\theta = 41.8^\circ$  in the spectrum was originated from the (006) plane of

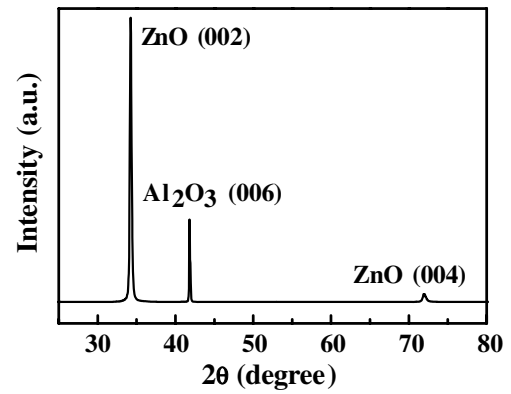


**Figure 2.** XRD spectrum of ZnO grown on the sapphire substrate by rf sputter.

the sapphire substrate. Such a result indicates that the ZnO film was preferentially grown in the  $c$ -axis direction.

Figure 3 shows current–voltage ( $I$ – $V$ ) characteristics of the fabricated ZnO Schottky diodes. For forward bias and  $V > 3kT/q$ , the following equation describes the  $I$ – $V$  characteristics of the Schottky diode according to the thermionic emission theory:

$$J = J_S [\exp(q(V - IR_s/nkT)) - 1], \quad (1)$$

$$J_S = A^* T^2 \exp(-q\phi_B/kT),$$

where  $k$ ,  $T$ ,  $R_s$ ,  $n$ ,  $A^*$  and  $\phi_B$  are Boltzmann's constant, absolute temperature, series resistance, ideality factor, effective Richardson coefficient and barrier height, respectively. Here, we assumed  $A^* = 4\pi qm^*k^2 h^{-3}$  and  $m^* \sim 0.27m_0$  [11] so that  $A^* \sim 32 \text{ A cm}^{-2} \text{ K}^{-2}$ . Furthermore, we can obtain the following equation from equation (1):

$$\frac{dV}{d(\ln J)} = JSR + \frac{n}{\beta}, \quad (2)$$

where  $\beta = q/kT$ ,  $S$  is the contact area. Thus, the plot of  $dV/d(\ln J)$  versus  $J$  will give a straight line with slope  $SR$  and the  $y$ -axis intercept  $n/\beta$ . Hence the ideality factor  $n$  was determined to be 1.68 [19].

In order to evaluate  $\phi_B$ , we then defined a function  $H(J)$  from equation (1) as follows:

$$H(J) = JSR + n\phi_B, \quad \text{where} \quad (3)$$

$$H(J) \equiv V - \frac{n}{\beta} \ln \left( \frac{J}{A^* T^2} \right).$$

Using the  $n$  value determined from equation (2), the plot of  $H(J)$  versus  $J$  will also give a straight line while the  $y$ -axis intercept is equal to  $n\phi_B$ . Figure 4 shows  $H(I)$  as a function of  $I$ , where  $I$  is  $JS$ . It can be found that the intercept value was 1.38 by the calculation. Then the Schottky barrier height between Ir and ZnO was found to be  $0.824 \pm 0.04\% \text{ eV}$ .

In this study, we also adopt the Nord method [20] to obtain the value of  $\phi_B$  by plotting the  $F(V)$ – $V$  curves. The

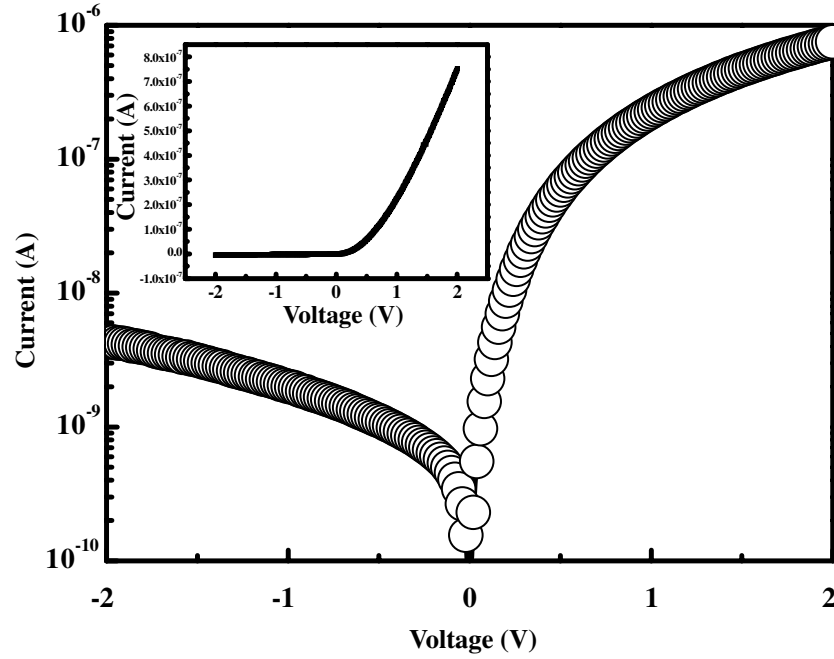


Figure 3.  $I$ - $V$  characteristics of the fabricated ZnO Schottky diodes. (inset: linear scale)

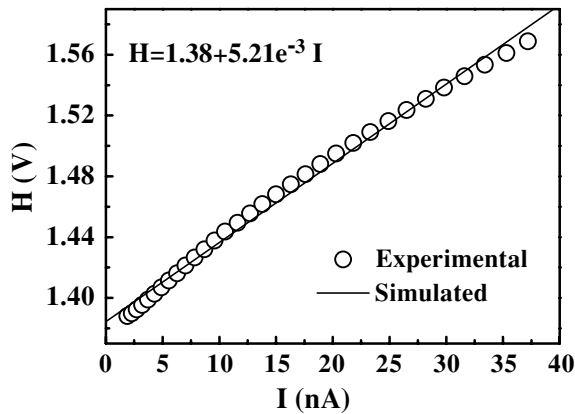


Figure 4. The experimental and simulated  $H(I)$  versus  $I$  plot of ZnO Schottky diodes.

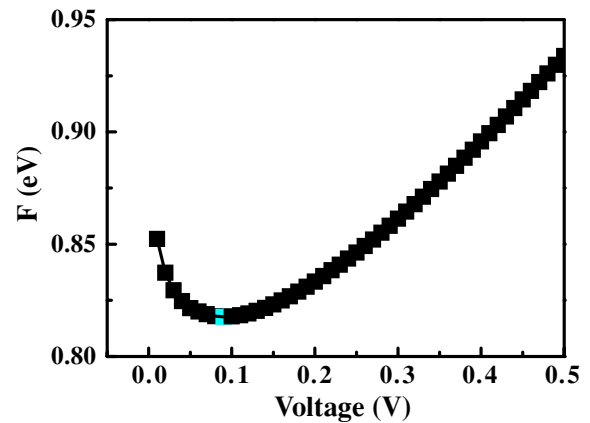


Figure 5. The  $F(V)$ - $V$  curve of the ZnO Schottky diode.

$F(V)$  function is defined as

$$F(V) = \frac{V}{2} - \frac{kT}{q} \left[ \ln \left( \frac{I(V)}{SA^*T^2} \right) \right], \quad (4)$$

where  $I(V)$  originates from the  $I$ - $V$  curve. From the minimum of the  $F$ - $V$  curve, the effective Schottky barrier height can be expressed as

$$\phi_B = F(V_{\min}) + \frac{V_{\min}}{2} - \frac{kT}{q}, \quad (5)$$

where  $F(V_{\min})$  is the minimum point of the  $F(V)$  curve and  $V_{\min}$  is the corresponding voltage. Figure 5 shows the  $F(V)$ - $V$  curve of the ZnO Schottky diode. According to the  $F(V)$ - $V$  curve, the effective Schottky barrier height is estimated to be  $0.837 \pm 0.04\%$  eV.

The  $C$ - $V$  measurement was performed at 100 kHz. The Schottky barrier height was calculated by

$$\frac{1}{C^2} = \left( \frac{2}{\varepsilon q N_D S^2} \right) \left( V_{\text{bi}} - V - \frac{kT}{q} \right), \quad (6)$$

where  $S$  is the Schottky contact area of the diode, the permittivity  $\varepsilon$  for ZnO is  $9.0\varepsilon_0$  [11],  $V_{\text{bi}}$  is the built-in potential and all other symbols have their usual meanings. In this equation, it is assumed that the diode does not have an appreciable interfacial oxide layer and that the n-type semiconductor has a uniform donor concentration  $N_D$ . It can be seen that a plot of  $1/C^2$  versus  $V$  gives a straight line with slope  $-2/\varepsilon q N_D S^2$  and an intercept on the voltage axis  $V_0 = (V_{\text{bi}} - kT/q)$  by equation (6). The slope of the straight line can be used to determine the dopant concentration  $N_D$  and the built-in potential  $V_{\text{bi}}$ , then the barrier height  $\phi_B$  is obtained

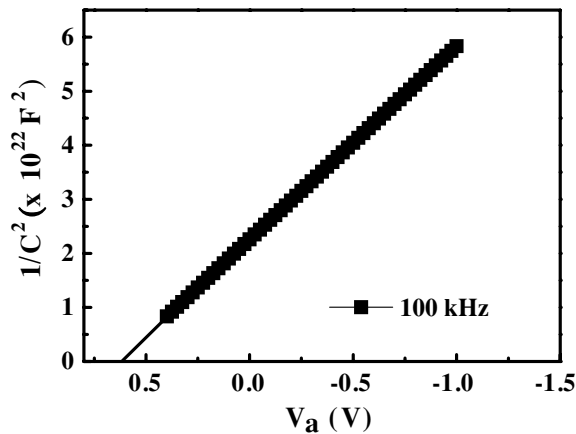


**Figure 6.**  $1/C^2$  versus the applied voltage curve of the ZnO Schottky diode measured at 100 kHz.

as

$$\phi_B = V_{bi} + \frac{kT}{q} \ln \left( \frac{N_C}{N_D} \right), \quad (7)$$

where  $N_C$  is the effective density of states in the conduction band. At room temperature, the theoretical value of  $N_C$  is calculated to be  $3.5 \times 10^{18} \text{ cm}^{-3}$  for ZnO [11]. As shown in figure 6, it can be found that  $V_{bi}$ ,  $N_D$  and  $\phi_B$  were determined to be 0.633 V,  $4.57 \times 10^{13} \text{ cm}^{-3}$  and  $0.924 \pm 0.04\%$  eV, respectively. The value of  $N_D$  extracted from the  $1/C^2$  versus  $V$  plot is similar to it measured from Hall measurement. This indicated the accuracy of our Hall measurement. The Schottky barrier height deduced from  $C-V$  method is slightly larger than the  $I-V$  method. This discrepancy might be due to the Schottky effect of the  $I-V$  method or closely related to the lower carrier concentration of our ZnO film.

#### 4. Summary

In summary, Schottky diodes with iridium contact electrode on ZnO films were fabricated and characterized in this work. The Schottky barrier height between Ir and ZnO was determined to be  $0.824 \pm 0.04\%$ ,  $0.837 \pm 0.04\%$  and  $0.924 \pm 0.04\%$  eV by thermionic emission model, Norde model and capacitance-voltage measurement, respectively. The ideality factor was also found to be 1.68.

#### Acknowledgment

This work was supported by National Science Council of Taiwan under contract numbers NSC-95-2215-E-150-077-MY3 and NSC-95-2622-E-150-031-CC3.

#### References

- [1] Barnes T M, Leaf J, Hand S, Fry C and Wolden C A 2004 *J. Appl. Phys.* **96** 7036
- [2] Kato H, Sano M, Miyanoto K and Yao T 2003 *Japan J. Appl. Phys.* **42** L1002
- [3] Alivov Y I, Kalinina E V, Cherenkov A E, Look D C, Ataev B M, Omaev A K, Chukichev M V and Bagnall D M 2003 *Appl. Phys. Lett.* **83** 4719
- [4] Liang S, Sheng H, Liu Y, Huo Z, Lu Y and Shen H 2001 *J. Crystal Growth* **225** 110
- [5] Mang, Reimann K and Rübenaacke St 1995 *Solid State Commun.* **94** 251
- [6] Setiawan, Vashaei Z, Cho M W, Yao T, Kato H, Sano M, Miyamoto K, Yonenaga I and Ko H J 2004 *J. Appl. Phys.* **96** 3763
- [7] Kaidashev E M, Lorenz M, von Wenckstern H, Rahm A, Semmelhack H C, Han K H, Benndorf G, Bundesmann C, Hochmuth H and Grundmann M 2003 *Appl. Phys. Lett.* **82** 3901
- [8] Sakurai K, Iwata D, Fujita S and Fujita S 1999 *Japan J. Appl. Phys.* **38** 2606
- [9] Ko H J, Chen Y F, Hong S K and Yao T 2000 *J. Crystal Growth* **209** 816
- [10] Pintilie L and Pintilie I 2001 *Mater. Sci. Eng. B* **80** 388
- [11] Sheng H, Muthukumar S, Emanetoglu N W and Lu Y 2002 *Appl. Phys. Lett.* **80** 2132
- [12] Ip K, Heo Y W, Baik K H, Norton D P, Pearton S J, Kim S, LaRoche J R and Ren F 2004 *Appl. Phys. Lett.* **84** 2835
- [13] Mosbacher H L, Strzhermechny Y M, White B D, Smith P E, Look D C, Reynolds D C, Litton C W and Brillson L J 2005 *Appl. Phys. Lett.* **87** 012102
- [14] Angadi B, Park H C, Choi H W, Choi J W and Choi W K 2007 *J. Phys. D: Appl. Phys.* **40** 1422
- [15] Kim J K, Jang H W, Jeon C M and Lee J L 2002 *Appl. Phys. Lett.* **81** 4655
- [16] Kim J K and Lee J L 2004 *J. Electrochem. Soc.* **151** G190
- [17] Jang H W and Lee J L 2003 *J. Appl. Phys.* **93** 5416
- [18] Maeda K, Mitsuru S, Ikuro N and Tsuguo F 2005 *Semicond. Sci. Technol.* **20** S49
- [19] Cheung S K and Cheung N W 1986 *Appl. Phys. Lett.* **49** 85
- [20] Norde H 1979 *J. Appl. Phys.* **50** 5052